Eur. Phys. J. D **14**, 191–203 (2001)

THE EUROPEAN PHYSICAL JOURNAL D

EDP Sciences

Femtosecond to nanosecond relaxation time scales in electronically excited tetrakis(dimethylamino)ethylene: identification of the intermediates

B. Soep[a], J.M. Mestdagh[b], S. Sorgues[a], and J.P. Visticot

Laboratoire Francis Perrin[c], CEA/DRECAM/Service des Photons, Atomes et Molécules, C.E.N. Saclay, 91191 Gif-sur-Yvette Cedex, France

Received 17 January 2001 and Received in final form 23 February 2001

Abstract. In the TDMAE molecule (title molecule), the time evolution has been analyzed from the very initial excitation step down to a fluorescent state, over widely different time scales. Pump probe measurements have been performed at 3 different excitation wavelengths 400, 266 and 200 nm. The decay has been followed over the femtosecond and subnanosecond ranges with this method and the decay of the final charge transfer state has been detected by its fluorescence emission. This allows an overview of the complete decay mechanism. The initial relaxation pathway is interpreted in a similar way to ethylenic molecules, where the initial wavepacket is quickly trapped in a doubly excited state Z with charge transfer character. Then the Z state decays slowly (10–100 picoseconds) into the final state. In difference to monoalkenes the final stage of this evolution is a charge transfer state. The decay of transient Z state to the charge transfer state is a further assessment of the partial ionic character of the Z state. This type of molecule with low ionization potential can be viewed as a demonstrative example of the interrelation between the charge induced forces and the deformations in excited state reaction dynamics.

PACS. 33.50.-j Fluorescence and phosphorescence; radiationless transitions, quenching (intersystem crossing, internal conversion) – 34.30.+h Intramolecular energy transfer; intramolecular dynamics; dynamics of van der Waals molecules – 34.50.Gb Electronic excitation and ionization of molecules; intermediate molecular states (including lifetimes, state mixing, etc.) – 82.53.-k Femtochemistry

1 Introduction

The detection of ultrafast relaxation in molecules is a new outcome of femtochemistry where ultrashort lasers have allowed the observation of processes involving direct wavepacket motion through barrierless potential energy surfaces [1–8]. The passage between excited potential energy surfaces of polyatomic molecules *via* the funnels created by conical intersections, causes a radiationless decay at the rate of molecular motions, thus much faster than that provided by the radiationless transition mechanism. The latter mechanism has been described in the theory developed by Jortner *et al.* [9]. Two electronic states are coupled by non adiabatic terms. The coherent optical excitation creates a nonstationary state, superposition of the coupled levels, which evolves into the final state, by decay of their coherence. This evolution can be viewed as a tunneling between non intersecting initial and final states; its rate is determined by a Fermi golden rule law [9] involving the density of final states and coupling matrix elements. Given the very small value of the coupling elements, the resulting rate is small as compared to the vibrational frequencies of the molecular states. This theory accounts well for the radiationless decay in the situation of distant, non crossing potential energy surfaces whose interacting states are weakly coupled *via* non adiabatic terms. It is replaced by a direct wavepacket movement when the states are allowed to cross through conical intersections. We can thus categorize two extreme situations: the first one where the timescale associated to such a mechanism is quite long, in the order of a few tens or hundreds of picoseconds, since it involves many vibrational periods of the system before substantial flux is transferred *via* the regions of maximum coupling in the surface. The opposite situation is encountered when a direct route exists between the initial and the final states. In that case, femtosecond timescales are observed that are associated with wavepacket movements through funnels connecting the initial and final states. The concept of funnels connecting surfaces *via* conical intersections is quite old [10–12], but it has regained a second life

[a] *Present address:* CNRS/Laboratoire de Photophysique Moléculaire, Université Paris-Sud, 91405 Orsay, France.
[b] e-mail: jmm@drecam.saclay.cea.fr
[c] CNRS-FRE-2298

in the recent years, essentially because it allows for a free motion between different electronic surfaces [13]. The evidence for this mechanism stems from quantum chemistry calculations which show the ubiquitous presence of these intersections [14,15] and from experiments showing the ultrafast relaxation in a variety of molecules [16–20].

As a general phenomenon, in ethylenic compounds, a very rapid internal conversion to the ground state occurs by a direct mechanism involving wavepacket motion over the potential energy surfaces of at least three electronic states, the optically excited state, V, a dark doubly excited state, Z and the ground state N [2,20–24]. These states are directly connected *via* conical intersections that ensure direct motion from one to the other. This motion involves several coordinates that generate severe deformation of the molecule: the central twist on the double bond, the pyramidalization of the adjacent carbon bonds, or H atom migration [2,20,22,24–26]. These deformations allow the surfaces to intersect and are generic to ethylenic compounds. In this relaxation model the excitation brings a wavepacket on the valence state (V), with a steep potential energy gradient along the C–C torsional coordinate, it crosses the intersection to the dark doubly excited (Z) state with zwitterionic character (note that a distinction will be made in the following between a Z state and a charge transfer state noted CT). There, the wavepacket is trapped in the Z state by further evolution on other coordinates, pyramidalization of the carbons or H migration and goes through another crossing to the ground state (N).

The purpose of the present paper is to explore the complete evolution on femtosecond and picosecond time scales from the Franck-Condon excited region of an ethylenic derivative, tetrakis (dimethylamino) ethylene (TDMAE), down to a final state from which it fluoresces to the ground state at a nanosecond time scale. The existence of this state makes TDMAE different from the other monoalkenes we have studied so far [20]. Experiments were run also, to measure the fluorescence lifetime of this state. Of course, the present work intends to interpret this evolution, as caused by the same kind of forces as in the alkene case, acting within similar states. The very interesting perspective offered by this molecule is that the two radiationless processes mentioned above, the rapid one and the slow one are both in play to account for the full excited state dynamics of the molecule. The response of the molecule will be studied for a variety of initial energy deposition ranging between 3.1 and 6.2 eV, 3.1 eV being only slightly above the final state energy, whereas 6.2 eV is larger than the ionization energy of the molecule.

2 Experimental

2.1 Real-time experiments

The experimental apparatus used for the real-time experiments associates a pulsed supersonic beam of TDMAE seeded in helium with a Time-Of-Flight Mass-Spectrometer (TOF-MS) and a Time-Of-Flight Photoelectron-Spectrometer (TOF-PE). It is coupled to the LUCA femtosecond laser facility of Saclay, in order to perform pump-probe experiments.

The LUCA laser facility delivers pump and probe pulses of two different colors. We have chosen to use the fundamental of a titanium-sapphire regenerative amplifier at 800 nm, with a 20 Hz repetition rate, as the probe. We have varied the energy of the 800 nm pulse between 15 μJ and 150 μJ with a mild focusing on a 0.5 mm diameter. The typical operating conditions correspond to a laser intensity of 2×10^{11} W cm^{-2}, which is deemed to achieve sufficiently low field ionization [27,28]. This is further discussed in Section 3.2. The pump is achieved either by the quadrupled (200 nm), tripled (266.7 nm) and doubled (400 nm) outputs of the titanium-sapphire. The harmonics input of the laser is passed through a delay line, which allows us to vary the time delay between them (the pump) and the 800 nm laser pulses (the probe). Positive times correspond to the probe pulse coming after the pump pulse. The pump and probe laser beams are collinear, and are slightly focused in the extraction zone of the TOF-MS/TOF-PE, where they cross the molecular beam, perpendicularly.

The general setup has been reported in a previous experiment [20]. Importantly, we derive additional information here by detecting the photoelectrons from ionized TDMAE. This is performed in a time of flight set up (the TOF-PE spectrometer) with a 50 cm flight path. For increased sensitivity the electrons are extracted by a 1 V voltage. In such circumstances the electron TOF has to be calibrated, this is performed in the following way: the flight time of zero kinetic energy electrons has been measured as a function of the extraction field. This yields the time *versus* energy relation for the electron movement. The applied extraction voltage, generally 1 V, will be deduced from the derived kinetic energy. The resolution of such a device is *ca.* 150 meV only, but sufficient in our experiment.

The pump laser performs a single photon excitation of the TDMAE molecule, and the resulting excited system is ionized by the probe with one or two photons. Fragmentation of the resulting ion may occur, and therefore both parent and fragment ions are detected, using the TOF-MS. A PC-computer allows us to record either the ion signals at various masses, or the electron signal as a function of the time delay between the pump and probe pulses.

The supersonic beam source enables to co-expand a mixture of He with TDMAE. The gas mixture is performed in the fore-line of the molecular beam. Commercial TDMAE from Aldrich is employed with no further purification, but after thorough outgassing. The beam is operated with a helium backing pressure in the fore-line of typically 1.5 bar. The expansion proceeds through a 0.1 mm nozzle, with an opening time of the pulsed valve of 160 μs.

Room temperature experiments are performed also, by introducing pure TDMAE through a needle valve inside the ionization region of the TOF mass spectrometers. The operating pressure was typically 10^{-6} mbar in this case. This arrangement is useful in the case of low signals to

still get some information on the time evolution of the molecule, at room temperature. It can also be used to check for the influence of clusters in the decays, especially in the case of long non exponential decays, room temperature TDMAE is indeed free of clusters.

The zero time delay between the pump and probe laser pulses has been determined in each experiment by reference to butadiene which displays an ultra-short decay. The time evolution of the butadiene ion was measured in a pump-probe experiment as 20 fs, by comparison with that of ammonia, 39 fs [20,29]. The cross-correlation of the laser pulses has typically a 180 fs FWHM with the 200/800 nm pump/probe arrangement, 140 fs for 266/800 nm and 100 fs for 400/800 nm. The position and width of the cross correlation function is adjusted to get a good fit of the butadiene signal, which determines the time resolution of the experiment as well as the zero time delay between the pump and the probe pulses.

2.2 Measurement of fluorescence lifetimes

Fluorescence measurements are performed, using a different supersonic beam machine. A nanosecond dye laser operating at either 266, 286 or 400 nm is used to excite the molecule in the free jet expansion of a TDMAE/He mixture, at 60 diameters from the nozzle. The fluorescence is observed with an Hamamatsu R15640U ultrafast photomultiplier tube and recorded as a function of the time with a 9362 Lecroy 1.5 GHz digital oscilloscope.

2.3 Data analysis in the real-time experiments

The decay patterns of most of the transient species follow a sequential scheme where a rapid transient is continued by a slowly decaying signal, as the delay time between the pump and the probe is increased. The relative height of both contributions varies considerably from one pump/probe situation to the other.

Such multiple decays are extremely common in femtosecond experiments. A rather general and complicated kinetic model is used in the appendix of reference [17] to help interpreting experimental data. Another one is given in references [3,30], which offers the possibility of having several probing sites along the reaction coordinate. The latter one is used here under the simple form where the system can be probed at two locations A and B. The initially populated level A decays into level B at rate $k_A = 1/\tau_A$ and B decays into C at rate $k_B = 1/\tau_B$ [20]. Let a and b be the efficiency for probing levels A and B (proportional to their ionization cross-section). A zero probe efficiency of level C is assumed under most of our experimental conditions. In the discussion, we shall interpret A as the initially populated Franck-Condon region, B as an intermediate electronically excited region of the parent molecule and C as the final state which will be identified as the light emitting charge transfer state of TDMAE.

This simple kinetic model corresponds to $k_d = 0$ in reference [17], with the following correspondence $k_{IVR} \rightarrow k_A$ and $k_i \rightarrow k_B$. Compared to the kinetic model of reference [3], quantities τ_1 and τ_2 are merged here into τ_A (we could not distinguish between them with the resolution of the present work) and τ_3 in [3] corresponds to the present τ_B. This model leads to the following expression for the signal $S(t)$, where $S(t)$ appears as a sum of the ionization signals from the populations of A and B, while a and b represent the ionization cross-sections of A and B:

$$S(t) \propto a \exp\left(-\frac{t}{\tau_A}\right) + b\frac{\tau_B}{\tau_B - \tau_A} \times \left[1 - \exp\left(-t\left(\frac{1}{\tau_A} - \frac{1}{\tau_B}\right)\right)\right] \exp\left(-\frac{t}{\tau_B}\right) \quad \text{for} \quad t > 0,$$
$$S(t) = 0 \quad \text{for} \quad t \leq 0. \tag{1}$$

The resulting $S(t)$ is convoluted with the cross correlation width of the lasers and the best fit with the experimental signal leads to the determination of both τ_A and τ_B.

3 The TDMAE molecule; pump-probe schemes

3.1 The tetrakis(dimethylamino)ethylene molecule (TDMAE)

Not too much is known on the spectroscopy and structure of the TDMAE molecule. The scattered information available on this molecule is collected below.

Ground state TDMAE

Ground state TDMAE has the general formula:

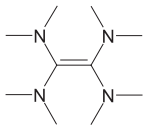

Owing to the C=C double bond, ground state TDMAE would be expected to be quasi planar. However, a deviation by 28° from planarity is predicted [31], due to the mutual repulsion of the bulky adjacent CH_3 groups. This is shown on the scheme at the bottom left corner of Figure 1, as a rotation of angle β about the CC bond. In addition, the nitrogen bonds are not pyramidalized and the methyl groups are, most likely, in planes strongly twisted from the average plane of the molecule. The nitrogen lone pairs are twisted therefore by 55° out of their optimum π-interaction with the C=C double bond [31]. A recent calculation by Fleurat-Lessard and Volatron predicts two geometries of equivalent energy because of a compensation between electronic and steric effects. One minimizing the steric hindrance is close to that mentioned above, the other one, more favored electronically, is less tilted about the C=C bond [32]. Under our experimental conditions where low temperature TDMAE is generated in the supersonic expansion, the isomer minimizing the steric effect might be the most populated.

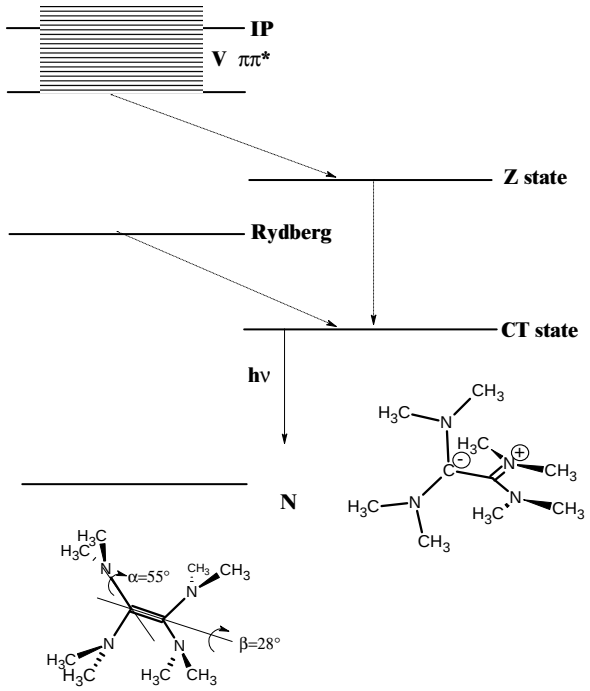

Fig. 1. TDMAE: schematics of the levels and structures [32].

Excited valence and Rydberg states of TDMAE

The absorption spectrum of gas phase TDMAE was measured at room temperature by Nakato *et al.* [33]. It is shown in Figure 2. The absorption is dominated by Rydberg transitions, likely $3s \leftarrow$ N at low photon energies. It is superimposed on the broad absorption of the valence $\pi-\pi^*$ transition whose maximum lies at 52 000 cm^{-1}, above the adiabatic ionization limit of the molecule located at $\sim$ 44 000 cm^{-1}($\sim$ 5.4 eV) [33]. The presumed $\pi-\pi^*$ transition is extremely broad with a similar location and extension as in the ethylene molecule, implying a profound geometry difference with the ground state of TDMAE. The relative positions of the V and R states, with respect to the ions level are shown in Figure 1.

To complement this information, we have independently investigated the absorption spectrum of TDMAE by nanosecond two-photon, single color ionization, near the origin of the absorption band, at 400 nm. The corresponding spectrum is shown at the bottom of Figure 2. It is intrinsically diffuse. Its width at half maximum of *ca.* 450 cm^{-1} indicates the presence of a very rapid relaxation process, in the order of 10 fs. One can note however that in Nakato's spectrum at the top of Figure 2, the apparent diffuseness of the states (Rydberg) decreases notably with increasing photon energy.

The TDMAE ion

The Rydberg series decrease in intensity with increasing number (the typical dependency is $1/n^3$) and merge into the ionization threshold. This ionization threshold has been measured in the gas phase and lies at 5.4 eV [33].

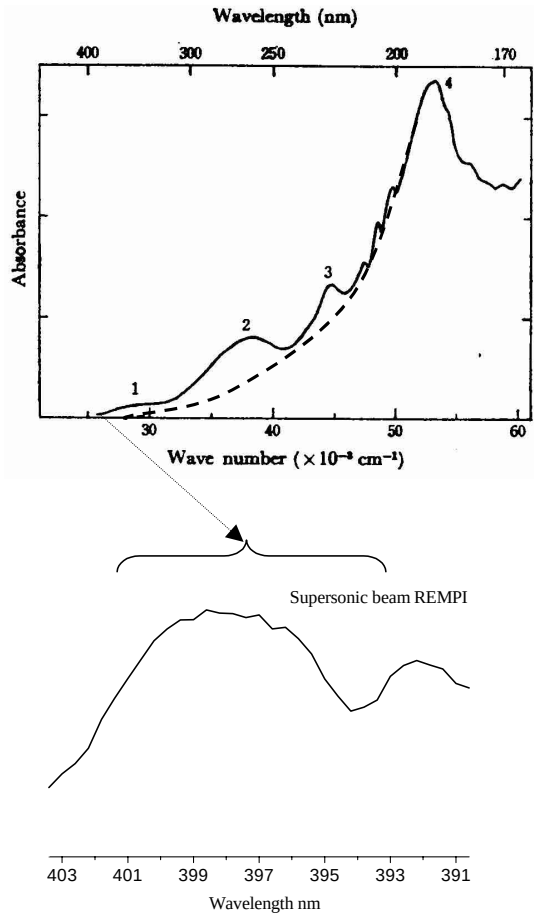

Fig. 2. From top to bottom: absorption spectrum of TDMAE in the gas phase, adapted from Nakato [33], the Rydberg progression labeled 1, 2, 3 converges towards the IP at 5.4 eV. The contribution of the $\pi-\pi^*$ transition is indicated by a dashed line and the maximum is labeled 4. Bottom: enlarged view of the origin band 1, as measured in the present work by the resonant two photon ionization in a supersonic beam.

Also photoelectron spectra performed with a helium lamp confirm the existence of a very low ionization potential at *ca.* 5.5 eV exhibiting for the ground state of the ion a diffuse spectrum that merges into a low lying excited state 1.5 eV above it [34]. One might assign this threshold to the ejection of an electron located on the highest π molecular orbital centered on the central C–C bond. This threshold would however be too high in energy, typically 8 eV in monoalkenes. Rather we infer that such a low value (5.4 eV) corresponds to an electron ejected from an orbital located around the nitrogen atoms, thus allowing for a delocalization of the positive charge on the four nitrogen atoms, according to:

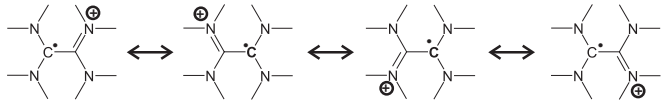

This structure allows indeed for an important stabilization of the ion.

The ethylenic $\pi\pi^*$ strong absorption maximum at 190 nm is continued by a strong absorption at shorter wavelengths well above the ionization potential [33]. This absorption lies in the Rydberg region of ethylene. The equivalent Rydberg series for TDMAE should converge to a higher ionization energy than 5.4 eV, such as the above mentioned one.

Zwitterionic and charge transfer state of TDMAE

By similarity with other ethylenic compounds, we shall infer the existence of a doubly excited state Z in the TDMAE molecule that can be displayed in the following way, as it possesses a sudden polarization character:

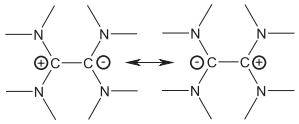

This state is dark, being doubly excited, but, there are probably many other dark states in this energy region, whose presence and role could be characterized helpfully by quantum chemistry calculations.

The TDMAE molecule is rich in electrons through the nitrogen atoms connected with the double bond. Hence the Z state which is in ethylene a superposition of two equivalent resonant structures with positive and negative carbons, is expected to have developed here into two states. One (Z) will be the in-phase combination and the other (CT) the out of phase combination. The CT state can be further stabilized as:

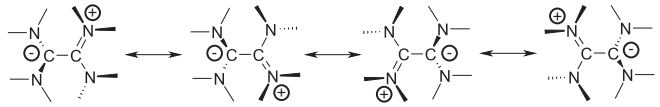

Owing to the rupture of the CC double bond, it can be inferred that the equilibrium structure of the CT state is strongly twisted, as shown at the lower right corner of Figure 1.

Emission that could be assigned to the CT state has been observed both in the gas [35] and in liquids [36,37]. The basis for this assignment relies on solvent effects with different electron accepting capabilities, where an electron accepting solvent captures an electron from the negative carbon of the CT state of TDMAE. The typical emission is broad, diffuse and strongly displaced from the absorption. It peaks at 487 nm (2.5 eV) in the gas phase and is displaced in polar solvents such as tetrahydrofuran, up to 570 nm. This has been interpreted as an emission by a donor($TDMAE^+$)-acceptor($solvent^-$)complex. From the similarity of the emission spectra in mildly acceptor solvents and in the gas phase, at 487 nm, we assume that the latter emission relates with an internal charge transfer state. It is difficult to assign with much confidence the origin of the oscillator strength in the charge transfer state which should be intrinsically small: strong mixing with the neighboring Rydberg state or mixing with the allowed transitions of the tertiary amino groups, which have known oscillator strength but lie higher in energy. Also the lone pairs from the nitrogen atoms, being tilted at 55° can only weakly contribute to the emission probability [36]. The resulting fluorescence lifetime, measured in tetramethylsilane liquid is 14.1 ns [37], a moderately long fluorescence lifetime compatible with intensity borrowing.

Such twisted internal charge transfer states are common in somehow different contexts. Twisted CT states are often observed in solutions [38] and in clusters of molecules, like DMABME with solvent molecules like CH_3CN [39]. There has been an abundant literature [38] describing the passage from the neutral locally excited state to the charge transfer that is deemed to imply a substantial twisting of the substituting groups on the molecule. However, in these molecules, the nature of the states involved is different from here, the TICT state not being connected with a doubly excited state as the Z state here. Also the very low ionization potential of TDMAE (5.4 eV) [33], allows for the existence of a charge transfer state in absence of solvent.

3.2 Pump-probe schemes

The temporal evolution of excited TDMAE has been observed in several pump probe schemes which correspond to different types of transitions in the molecule.

We have used the harmonics of the titanium-sapphire laser to excite the molecule TDMAE at 400.0 nm, 266.7 nm and 200.0 nm and probe with 800 nm photons. At 400 nm the 0–0 transition is reached, at 266 nm an intense transition is excited, likely a Rydberg superimposed on the leading edge of the $\pi-\pi^*$ transition [33]. At 200 nm (6.2 eV) the molecule is above the adiabatic ionization energy (5.4 eV) at the maximum of the $\pi-\pi^*$ region. Here too, it has probably also a quite important Rydberg character.

We have chosen the 800.0 nm probe, with the laser maintained in the range of 50 μJ giving an $\approx 2 \times 10^{11}$ W cm^{-2} intensity. It was checked by observing the photoelectron spectrum in a zero time delay experiment on butadiene that these conditions are well below the onset of above threshold ionization processes (ATI) due to the probe laser. Turning back to TDMAE, the photoelectron spectra shown in Section 4.2 indicate clearly that the ionization path does not imply ATI processes: high kinetic energy electron above 1.5 eV are indeed absent. Of course, under these intensity conditions, the probe alone does not generate any ion.

In all pump-probe schemes, the transients correspond to dynamics in the excited state neutral molecule. When the pump frequency is lower than the ionization energy of TDMAE, its intensity was adjusted to prevent multiphoton ionization. Therefore, as the probe does not produce any ion by itself also, the reported signals thus correspond to pure pump-probe signals documenting the excited state dynamics of neutral TDMAE. When the pump is tuned to

200 nm, *i.e.* above the ionization limit of TDMAE, the observed transient increase in the ion signal must arise from the ionization of an excited state of the neutral molecules. This will be more extensively discussed in Sections 4.1 and 5.3.

4 Results

The femtosecond and picosecond behavior of the free TDMAE molecule has been investigated following 200.0, 266.7 and 400.0 nm excitation. Fluorescence lifetimes following the 266, 286 and 400 nm excitations have been measured also. Clusters of TDMAE with itself and several polar and non-polar solvents have been investigated too, which results will be reported in a forthcoming paper.

4.1 200 nm excitation

This excitation is above the ionization energy of the TDMAE molecule and indeed the pump pulse provides a constant ionization signal by itself. However probing the state excited at 200 nm with light at 800 nm showed an increase in the ionization efficiency. As discussed in the literature, ionization at this wavelength has an efficiency of only 20% [40] and competes thus with other relaxation processes. These relaxation processes are overcome by excitation with the probe laser.

Observing photoelectrons

Photoelectron spectra of both pump only and pump probe signals have been recorded. Their structure is the following:

- the pump only signal peaks at low kinetic energy of the electrons. This is expected considering that the electrons originate from an autoionization process and that only 0.8 eV excess energy is available. Such signals are subtracted from the raw electron signals;
- the pump/probe signal is also peaked at low electron energy (≈ 0.1 eV), whatever the pump/probe delay.

Observing the parent ion

The transient observed when monitoring the parent TDMAE molecule is shown in Figure 3, top curve. The photoelectron signal when monitoring low energy electrons is not shown in the figure but exhibits the same 800 fs decay.

Observing fragment ions

Several fragment ions are observed. As apparent in Figure 4, fragments at masses 45, 57, 88 and 101 amu are observed besides the parent, which is the most abundant ion. It must be noted that the parent appears also at negative times *i.e.* in an ionization due to the sole pump laser. Instead, the fragments are observed only in a pump probe process except for a group of masses around 75 amu which has no connection with the process under study here. A probe intensity dependence of the fragment signals has been performed between 1 and 5×10^{11} W cm^{-2}. A linear increase of the fragment signal at mass 57 amu has been observed where the parent signal is constant. The slope of the intensity dependence implies that detection of this fragment needs one more photon than for the parent. The fragments of masses 45, 88 and 101 amu have a lower intensity dependence.

We infer that the 200 nm pump + 800 nm probe ionization yields fragment ions through disposal of a substantial excess energy excess (2.3 eV) in the parent ion TDMAE$^+$. Let us remark that the fragments have a higher power dependence with the probe laser than the parent, indicating a multiphoton process of higher order for their production than for the parent ion.

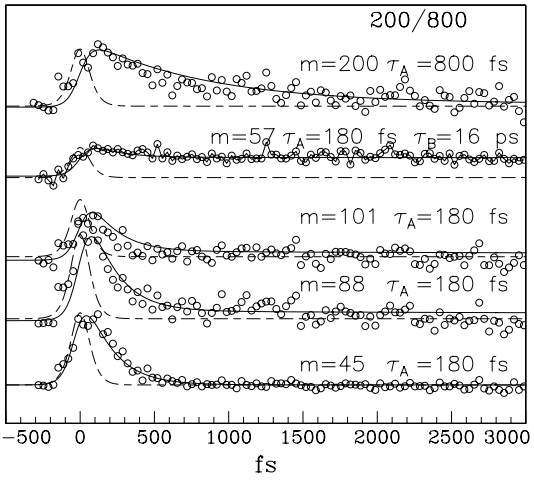

Fig. 3. Pumb probe detection of TDMAE$^+$ and fragments ions with 200 nm pump and 800 nm probe, as a function of pump/probe delay (fs). From top to bottom: parent at mass 200 amu and fragments at masses 57, 101, 88 and 45 amu.

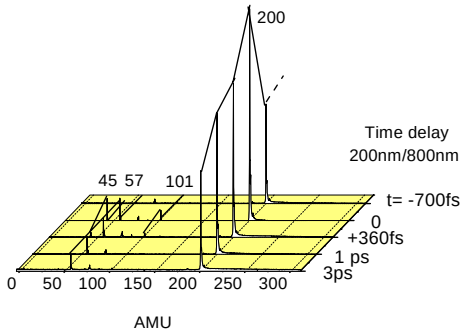

Fig. 4. Overview of the time dependent mass detection signals with 200 nm pump and 800 nm probe.

Table 1. Parameter τ_A and τ_B used in expression (1) to best fit the ion signals in Figures 3 and 6.

excitation wavelength (nm)	mass (amu)	rapid decay τ_A (fs)	slow decay τ_B (ps)
200	200	800	non measurable
	101	180	non measurable
	57	180	16
	88	180	no slow decay
	45	180	no slow decay
266	200	300	120

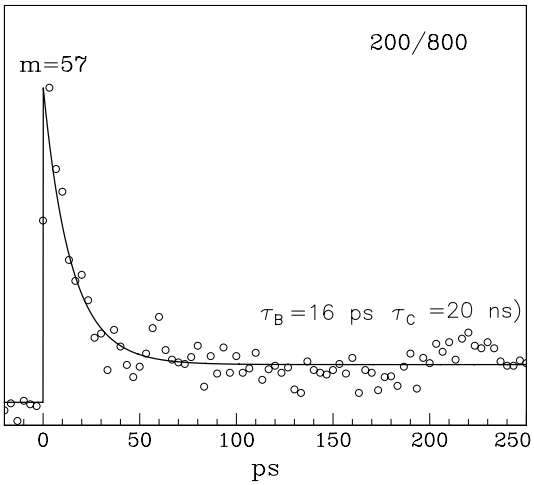

Fig. 5. Mass detection of the 57 amu fragment at a subnanosecond time scale with 200 nm pump and 800 nm probe.

The time dependencies of the fragment ion signals are shown in Figure 3, together with that of the parent $TDMAE^+$ ion. The parameters τ_A and τ_B used to fit the data of this figure are displayed in Table 1. The short decay time constant τ_A is larger for the parent than for the fragments (800 fs *versus* 180 fs). Moreover, the fragment at mass 57 amu has a measurable slow decay with a 16 ps time constant, when focusing the probe laser more strongly (see the probe intensity dependence of this signal in Sect. 4.1). The corresponding result is shown in Figure 5 up to a 250 ps delay time between the pump and the probe. In contrast, the other fragments have a single exponential decay.

4.2 266 nm excitation

With this excitation we reach a broad, intense band of the TDMAE molecule, which along Nakato's assignment lies at the edge of the $\pi\pi^*$ transition as represented in Figure 2.

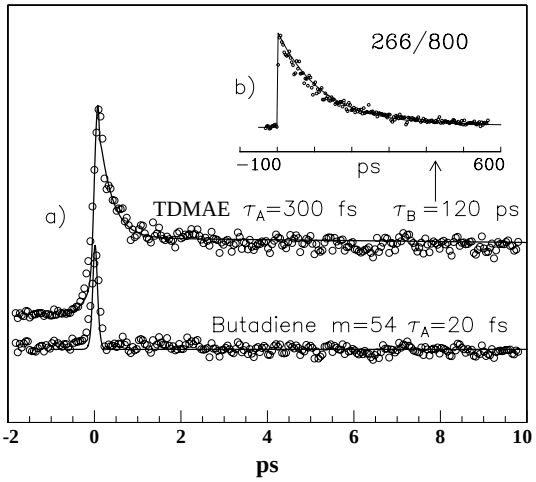

Fig. 6. Pump probe signal of the $TDMAE^+$ parent, compared with butadiene with 266 nm pump and 800 nm probe. In the insert, the decay of the $TDMAE^+$ parent is represented at much longer times, in the subnanosecond range.

Observing the parent ion

In contrast with the 200 nm observation, fragmentation is insignificant when exciting TDMAE at 266 nm. Hence, only the parent decay is represented in Figure 6. The corresponding parameters of the fit, τ_A and τ_B are given in Table 1. A short decay of 300 fs is followed by a slow one of 120 ps. With the scale of the figure, the slow decay appears as a plateau, but it has been followed over a few hundreds of picoseconds as shown in the insert of the figure. It must be noted that the pre-exponential factor of the longer decay exhibits a different power dependence with the probe laser than that of the short decay. This indicates that ionization proceeds through different schemes in both cases. This shows up again, when considering time dependent photoelectron spectra.

Observing photoelectrons

Photoelectron spectra taken at various pump/probe delays are shown in Figure 7. At time 0, *i.e.* at the maximum of the cross correlation between the pump and probe lasers, the intensity in the photoelectron spectrum peaks at zero kinetic energy but extends to higher values. The spectrum changes strikingly after the initial 300 fs decay and displays a double maximum, at $\sim$ 0 and 0.8 eV. The shape of the spectrum ceases to evolve at longer delay times, but its intensity decays with the same time constant of 120 ps as the parent ion signal.

Two cuts through Figure 7 are represented in Figure 8 that shows the time dependence of signals corresponding to $\approx$ 0 eV and 0.8 eV electrons. The 0 eV electron signal decays almost to zero in 300 fs. It contains a weak (5% of total) signal at negative times originating from a 800 nm multiphoton pump and a 266 probe which does not affect the fit at positive times. The maximum of the 0.8 eV electron signal is weaker than the 0 eV component,

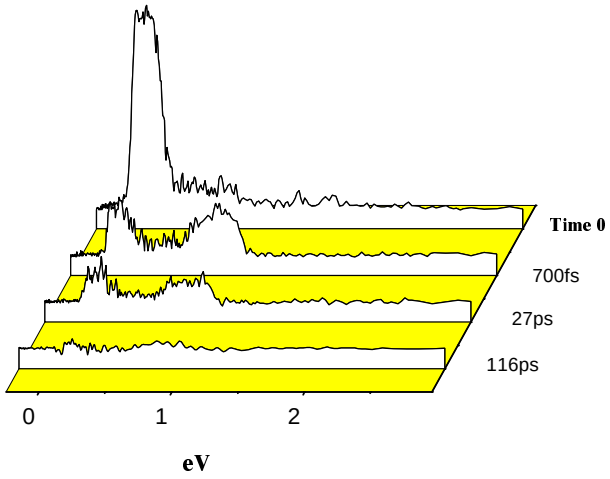

Fig. 7. Overview of the time resolved electron kinetic energy dependence of TDMAE in the 266 nm/800 nm pump probe scheme.

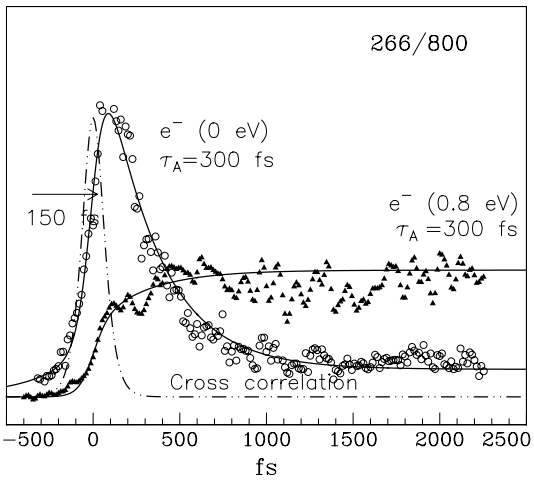

Fig. 8. Cuts of the time resolved electron kinetic energy dependence in Figure 7 at two energies $\sim$ 0 eV and 0.8 eV. The signal at 0.8 eV has been multiplied by a factor of 4. The cross correlation between the pump 266 nm and the probe 800 nm is indicated by a dashed line.

see Figure 7, and is contaminated up to 40% by it. After accounting for this contribution it can be observed that the 0.8 eV signal can be fitted with a 300 fs growth time as for the previous time constant. Figure 8 shows the experimental signal and the fit with the sum of contributions.

The signal associated with 0.4 eV electrons could have been drawn. It is not shown in the figure for clarity. It features a very rapid transient, almost identical to the cross correlation function of the lasers.

Finally, experiments have been run with room temperature TDMAE. The temporal characteristics of the decays are the same as those reported above for cold TDMAE in the supersonic beam. Internal energy is therefore not a parameter that affects dramatically the excited state dynamics of TDMAE, at least for the 266 nm excitation.

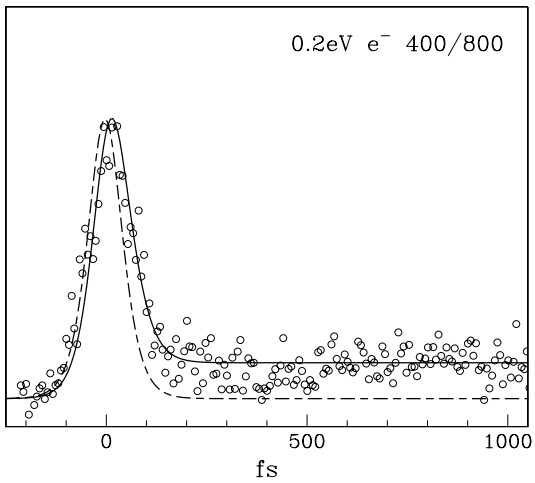

Fig. 9. Pump probe signal $TDMAE^+$ at 400 nm and 800 nm.

4.3 400 nm excitation

The time evolution of the parent TDMAE has been measured in the 400/800 pump-probe scheme. The signal is more than an order of magnitude weaker than in the above reported experiments. This was expected since we are exciting here a weak band, likely the origin of the TDMAE absorption spectrum. In order to get a significant pump probe signal both for ions and photoelectrons, we have been obliged to use the configuration where a room temperature static pressure (10^{-6} mbar) of TDMAE is introduced in the ionization zone of the TOF-MS.

No fragment is observed in this experiment. The signal corresponding to 0.2 eV photo electron signal is shown in Figure 9 as a function of the pump/probe delay time. The initial decay is extremely short and barely measurable ($\leq$ 20 fs). It is followed by a plateau or a very slow decay component, as in the 266/800 pump-probe scheme.

4.4 Fluorescence emission of TDMAE in supersonic jets

The separate experiment associating a supersonic beam and a nanosecond laser has allowed us to record the emission spectrum of TDMAE, exciting at 266, 286, 370 and 400 nm. It consists in a broad unstructured band centered at *ca.* 480 nm. The decay of the emission is well fitted by a single exponential with a 22 ns time constant when exciting the molecule at 266 and 286 nm, while it raises to 30 ns at 370 and 400 nm.

5 Discussion

The time evolution of the excited TDMAE molecule is characterized by three time scales: a femtosecond, picosecond and nanosecond one. The two first ones had been encountered already in our former study of monoalkene compounds [20]. We infer from the general relaxation

mechanism of ethylenic compounds discussed in this former work that the femtosecond evolution corresponds to a rapid wavepacket motion along deformation coordinates of the molecule. This motion is driven by steep potential gradients from the initially populated electronic state *via* a conical intersection to a lower electronic state that is assigned to Z, the zwitterionic state. The latter decays here, by non adiabatic coupling in a picosecond time scale, to a fluorescent state with a of lifetime in the ten nanosecond range. This excited state has no counterpart in the ethylenic compounds we have studied so far [20]. We anticipate that the fluorescent state is CT, the charge transfer state mentioned in Section 3.1. The existence of this state is the main difference with the ethylenic compounds: here instead of channeling the excitation into the ground state *via* a second conical intersection the excited molecule can be stabilized in an excited state whose geometry is far away from the intersections. However, we cannot state that all the flux from Z goes entirely to CT.

Issues in the present discussion is therefore to ascertain this general scheme. For this purpose, the dynamics of the TDMAE molecule, following the 266, 200 and 400 nm excitations is examined in finer details than just sketched above.

5.1 The CT state assignment

The lifetime of the fluorescent state has been measured in the present work, in the gas phase, under free jet conditions. It is weakly dependent on the energy of the excitation photon and varies between 22 ns at 260 nm and 30 ns at 400 nm. These values are comparable to that found in solution, 14.1 ns [37], given the relaxation and solvent effects in condensed media. Such a limited variation of the lifetime when the excitation energy varies on a range of 1.5 eV, indicates a similar final electronic state under both excitations, 260 and 400 nm. This is confirmed when observing the fluorescence spectrum. Whatever the excitation wavelength, 266, 286 or 400 nm, the free jet emission consists of the same broad band centered at 480 nm. Importantly, it matches the emission peaking at 487 nm observed in solution [35].

As mentioned in Section 3.1, the usual way of interpreting such large red shifts from the excitation is to assign the fluorescent state to a charge transfer state, CT. This state should undergo profound geometrical reorganization with the possible twisted geometry shown in Figure 1 and sketched below:

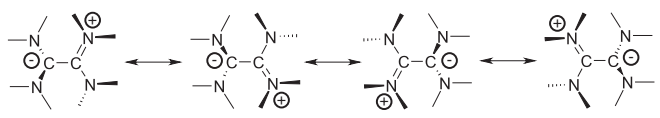

This represents fully charge transferred species. Of course a more elaborate representation would require partial charge transfer.

5.2 TDMAE dynamics after excitation at 266 nm

From Section 3 we know that excitation at 266 nm corresponds to a Rydberg transition superimposed on the *stronger* absorption edge of the valence $\pi\pi^*$ transition. A strong geometrical difference was anticipated between the valence state V and the ground state N of the TDMAE molecule.

We were able to characterize the evolution after the 266 nm excitation by two time constants, one short, 300 fs and a much longer one of 120 ps, by transient ionization measurements observing the parent ion $TDMAE^+$ and photoelectron spectra. As for the other monoalkenes, the shortest time constant should correspond to the wave packet motion on the potential energy surface connecting the accessed electronic state with a doubly excited state, the Z zwitterionic state in ethylenic language.

The initial movement responsible for the 300 fs decay is driven by the torque on the central C–C bond due to the difference in equilibrium geometry between the ground state N and the valence V state of the TDMAE molecule; this movement is probably coupled also to a change in the CC bond distance. The Frank-Condon region excited from the N state is indeed likely to correspond to a very distorted geometry in the valence state V. The 300 fs time constant corresponds to movement under this gradient (*i.e.* a rotation of angle β as shown in Fig. 1) plus the necessary rearrangements to change also the angle α about the C–N bond (see Fig. 1) and trap the wavepacket in the Z state.

The drastic switch of electronic configuration from V to Z during the first 300 fs is well illustrated by the evolution of the photoelectron spectra, as shown in Figures 7 and 8. For example in Figure 8, a simultaneous decay is observed for the low energy electrons accompanied by the rise of the higher energy ones. On the other hand, 0.4 eV electrons behave very much like the cross correlation function of the laser, indicating that they are due to a very rapid process. These observations give a key to resolve the dynamics of TDMAE at 266 nm into three steps:

1. departure from the Franck Condon region;
2. evolution towards the Z state;
3. the CT ← Z transfer.

Departure from the Franck Condon region

The excited TDMAE molecule is directly ionized as depicted in Figure 10 by a single 800 nm photon that brings the molecule over the adiabatic ionization energy with an excess energy of *ca.* 0.8 eV. Hence, given the energy resolution of the TOF-PE, the observation of 0.4 eV electrons appears as a good compromise to investigate this ionization scheme specifically, without contamination by electrons of 0 and 0.8 eV that have a different behavior. Since the corresponding signal essentially follows the cross correlation function of the laser, it may be concluded that the departure from the Franck-Condon region after excitation by the pump is very rapid. There are understandable reasons for that. At time zero, the molecule is

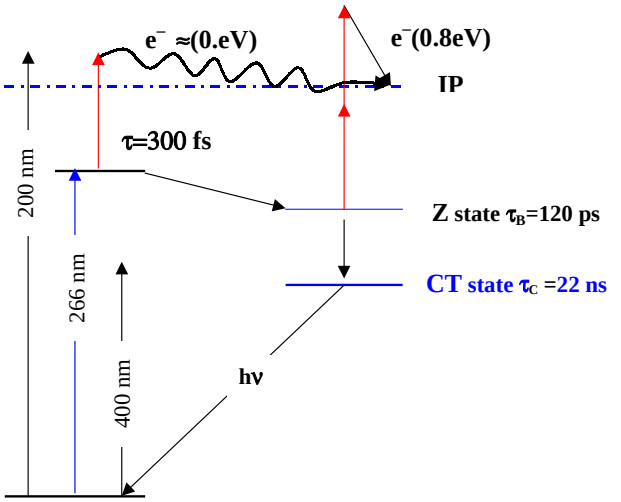

Fig. 10. Schematics of the pump probe excitation with 266 nm pump (also indicated the 200 and 400 nm exications).

in a strongly mixed Rydberg and valence state. A significant torque is applied about the central C–C bond because of the valence contribution. The resulting torsion with a large torque drives the molecule rapidly away from from the Franck-Condon region. Importantly, the torsion reduces the Rydberg character of the electronic state and therefore lowers dramatically the ionization efficiency of the molecule, in agreement with the experimental observation of nearly a cross correlation shape for the time dependence of the 0.4 eV electron signal.

Evolution towards the Z state

The wavepacket, which moves away rapidly from the mixed Rydberg-Valence (R-V) region, reaches the Z state in a no-return process through, most certainly, a conical intersection. The Z state is lower in energy, and also distorted with respect to the stable conformation of ground state TDMAE. As depicted in Figure 10 the large internal energy disposed in the Z states increases the ionization energy because of momentum conservation. It is conceivable that the increase in the ionization energy is large enough to necessitate a two photon process at 800 nm for the vertical ionization to proceed. Such assumption helps to account for the observations of Figure 7. Three points can be made:

- the two 800 nm photon ionization generates the new maximum in the photoelectron spectrum centered at 0.8 eV, after the 300 fs induction time. A similar ultrafast evolution in the photoelectron spectra has been observed for linear polyenes [18];
- the increase in the vertical ionization energy limits the electron energy to *ca.* 1 eV;
- the low efficiency of the two 800 nm photon ionization allows competition with the equally inefficient non vertical single photon ionization of TDMAE. This explains why both ≈ 0 eV and ≈ 0.8 eV electrons coexist with similar intensities at long time delays in the photoelectron spectra of Figure 7.

The Z state can tentatively be located ~ 2 eV below the ionization threshold (*i.e.* 3 eV energy above ground state), since photons with 3 eV energy (two 800 nm photons) yield electrons with 1 eV maximum energy.

The CT ← Z transfer

After the wavepacket motion towards the Z state, the excitation stays trapped in the Z state for 120 ps until it relaxes to the lowest fluorescent state, the charge-transfer state, CT. This decay is likely driven by weak non adiabatic couplings between the Z and CT states.

An energy transfer to such a CT state does not exist with the other monoalkenes we have studied so far [20]. Instead, a direct energy transfer of Z to the ground state N is observed with a time constant of a few picoseconds. Of course such a transfer appears to be blocked here, or if existing it would have a time scale much larger than 120 ps.

5.3 Excitation above the ionization limit at 200 nm

The absorption spectrum of TDMAE peaks at 190 nm (see Fig. 2). This corresponds likely to the maximum of the $\pi - \pi^*$ transition, but the corresponding excited state is expected to have a mixed valence and Rydberg character[1]. This absorption maximum is located above the adiabatic ionization threshold of TDMAE. Nevertheless, the ionization efficiency of TDMAE at 200 nm is only 20% [40] and 80% of the excited molecules remain in neutral states. This explains why a pump (200 nm)-probe (800 nm) signal could be observed in the present experiment, which documents the dynamics of excited neutral TDMAE. The observed signal increases by about a factor 2 after the action of the 800 nm probe (see Fig. 4). This can be understood as the excitation of an electron in the ion core followed by a very rapid autoionization. Indeed, an excited state of the $TDMAE^+$ ion exists at 1.5 eV, which allows for such a transition [34].

The 200/800 nm pump-probe signal has been monitored by following both the parent TDMAE ions and electrons of zero kinetic energy. The results are shown in Figure 3 and Table 1. A mono-exponential decay is observed with a time constant of 800 fs.

The fragment ions have also been monitored, see Figure 3 and the summary in Table 1. A different time behavior is observed as compared to the parent ion: the initial transient is shorter, 180 fs instead of 800 fs and too, the fragment of mass 57 amu has a slow secondary decay of 16 ps time constant. These results are extremely puzzling since the level apparently populated by the pump laser would simultaneously exhibit two different lifetimes, 180 and 800 fs whether the parent ion or its fragments are

[1] This Rydberg state belongs to a series converging to a higher limit most likely the π electron ionization.

observed. This is clearly impossible unless we suppose that the initially populated level is not the one which is actually probed. This would be the case in the following scenario, which seems the most probable. The pump laser excites the mixed Rydberg-Valence state, which could have an extremely short lifetime (less than 20 or 50 fs) caused by a rapid departure out of the Franck-Condon region. The time resolution of the present experiment cannot allow for observing such a rapid transient when superimposed to slower transients. Note that we have previously assigned a very short time constant to a Rydberg-Valence change in Section 5.2. This could happen here again, in a situation where the two different states, Rydberg and valence, are populated in an irreversible fashion by two different deformations. The subsequent dynamics is conceivably very different whether the valence or the Rydberg route is followed.

The valence route

After the 200 nm excitation and the rapid wavepacket motion which gives the dominant valence character to excited TDMAE, we can consider the molecule as a diradical. This is shown in the top left corner of the following scheme[2]:

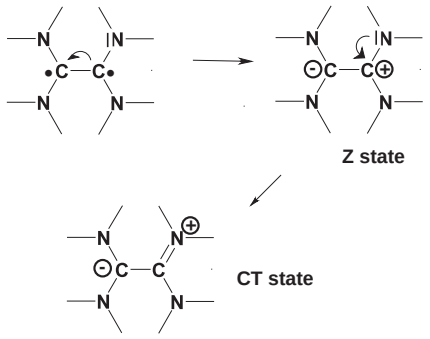

The subsequent wavepacket motion makes the electron of one singly occupied orbital on one carbon to transfer of the other carbon of the former CC double bond, thus leading to the zwitterionic state Z. This evolution is very much in the spirit of the evolution following the 266 nm excitation discussed in the preceding section. The difference is in the amount of energy given to the system: 6.2 eV in the 200 nm experiment, *versus* 4.6 eV with the 266 nm excitation. This energy difference, imparted to the neutral as internal excitation shows up as a more rapid evolution towards the Z state (180 fs *versus* 300 fs in the 266 nm experiment). It shows up also as a fragmentation of the TDMAE ion into masses 45, 57, 88 and 101 amu. Furthermore, after transferring into Z, TDMAE can be ionized in a two-photon process and fragments essentially into mass 57 amu[3]. This leads to the slow decay of 16 ps observed at mass 57 amu, indicating a lifetime of 16 ps for the Z state before transferring into CT, the charge transfer state. We should not be surprised to see this "short" lifetime here compared to the 120 ps found for the same state in the 266 nm experiment. This is another manifestation of the larger amount of energy deposited in the system when exciting at 200 nm.

The Rydberg route

The Rydberg state resulting from the 200 nm excitation and the subsequent rapid wavepacket motion, can be viewed as spatially diffuse. TDMAE then appears as a positive carbon core in TDMAE surrounded by a diffuse Rydberg electron.

This is schemed by the top left corner of the following scheme (see footnote 2):

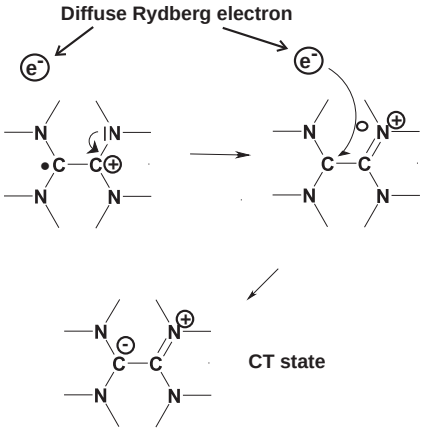

The positive carbon next to the free doublets on the nitrogen atoms cannot be stable for long after it has been formed. The ion core should rearrange to a more stable configuration with the positive charge delocalized on the nitrogen atoms, the other carbon, still having a lone electron (see top right corner of the above scheme). During this movement, if the Rydberg electron stays in an outer orbit, it is likely to be ejected after coupling with the ground state ion continuum. Such an autoionization mechanism might be partly responsible for ionization of TDMAE by 200 nm photons with the 20% efficiency. The Rydberg electron belongs to a a series localized close to the C–C bond, hence it can be stabilized also by forming a lone pair with the lone electron on carbon, making it negative. In that case, CT, the charge transfer state will be formed directly from the Rydberg state. In such a picture, the Rydberg state decays into CT with the experimental timescale of 800 fs.

[2] We think convenient to introduce schemes at this point, inspired by the description of reaction mechanisms in organic chemistry. The motivation is the existence of the final CT state, implying an electron flow. We must mention that such schemes give an idealized picture (without mesomeric forms) of the electron transfers driving the deformation of the molecule. These deformations induce in turn other electron movements. Of course the different time scales measured in the present work are dictated by the deformations of the molecule, and not by the electron movements.

[3] The signal at mass 57 amu has apparently about the same detectivity throughout the evolution from V to Z. Hence, no 180 fs transient shows up in the signal.

Substantial internal movement of the molecule is needed for both the evolution of the $TDMAE^+$ ion core and the Rydberg electron retrapping: rotation of angle β about the CC bond, rotation of angle α about the CN bonds, and pyramidalization about the carbon atom accepting the Rydberg electron. This explains the slow time constant of 800 fs which is associated with this route.

5.4 Excitation at 400 nm

The 400/800 nm pump/probe signal shown in Figure 9 is close to the cross correlation signal of the lasers indicating an ultrashort time evolution (20–50 fs). This is consistent with the diffuse single color two-photon ionization spectrum shown at the bottom of Figure 2 that would correspond to a *ca.* 10 fs evolution timescale following a 400 nm excitation. Again, such a timescale falls in the range encountered previously when discussing of the departure from Franck-Condon regions.

6 Conclusions

In the complex TDMAE molecule, the time evolution has been analyzed from the very initial excitation step down to a fluorescent state, over widely different time scales. This allows an overview of the complete decay. The relaxation pathway can be interpreted in a similar way to ethylenic molecules, where the initial wavepacket is quickly trapped in a doubly excited state with charge transfer character which continues to decay more slowly to the final state. Such zwitterionic states are elusive intermediates essential to characterize the excited state dynamics in ethylenic compounds. Here, the zwitterionic character of this intermediate state is consistent with its time dependent ionization properties. The time dependent photoelectron spectra exhibit a clear signature of this: the Z state is ionized by two 800 nm photons from an electron distribution and a geometry linked efficiently to the ion. The decay of the Z state into a lower charge transfer state is a further assessment of its charge distribution. In these experiments the molecule has been excited at three different energies spanning the domain from the origin band up to above the ionization limit. The observed decay features involve only a limited set of excited states: the Franck-Condon accessed state, Rydberg states, the zwitterionic state and the charge transfer state.

We have inferred a drastic change of geometry between the neutral TDMAE molecule and the ion where the central C–C bond twists in the ion at 90 degrees compared to the neutral, as shown in Figure 1 and the positive charge locates on a nitrogen. Likely the dimethyl amino groups also twists in this move. Thus the charge flow from the nitrogen to the central C–C bond locus of the excitation is accompanied by important geometrical changes. This type of molecules with low ionization potential can be viewed as a demonstrative example of the interrelation between the charge induced forces and the deformations in excited state reaction dynamics. Besides the existence of an excited state with very strong charge transfer character is rather seldom in organic molecules where solvent molecules are needed for their stabilization.

Hence solvent effect are sought here because a single polar solvent molecule can stabilize strongly and specifically such charge distributions. Indeed in a forthcoming work we shall report differences between the dynamics in non-polar solvents, polar solvents and hydrogen bonding solvents capable of stabilizing one structure. The charged intermediates or Rydberg states should be very sensitive to high intensity laser fields and some of the ionization properties may be related to "high" field properties, this is a domain that we shall now investigate.

The authors are happy to thank O. Gobert, P. Meynadier and M. Perdrix, who are responsible for developing, maintaining and running the femtosecond laser facility LUCA (Laser Ultra-Court Accordable) of the CEA, DSM/DRECAM. We also acknowledge financial support from ACI du MENRT Contrôle des réactions chimiques par laser.

References

1. C. Wan, M. Gupta, A.H. Zewail, Chem. Phys. Lett. **256**, 279 (1996).
2. W. Fuss, S. Lochbrunner, A.M. Muller, T. Schikarski, W.E. Schmid, S.A. Trushin, Chem. Phys. **232**, 161 (1998).
3. S.A. Trushin, S. Diemer, W. Fuß, K.L. Kompa, W.E. Schmid, Phys. Chem. Chem. Phys. **1**, 1431 (1999).
4. S. Zilberg, Y. Haas, Chem. Eur. J. **5**, 1755 (1999).
5. E.W.-G. Diau, S. De Feyter, A.H. Zewail, J. Chem. Phys. **110**, 9785 (1999).
6. E.W.-G. Diau, S. De Feyter, A.H. Zewail, Chem. Phys. Lett. **304**, 134 (1999).
7. W. Fuss, W.E. Schmid, S.A. Trushin, J. Chem. Phys. **112**, 8347 (2000).
8. A.H. Zewail, J. Phys. Chem. A **104**, 5660 (2000).
9. J. Jortner, S.A. Rice, R.M. Hochstrasser, Adv. Photochem. **7**, 149 (1969).
10. H.E. Zimmerman, J. Am. Chem. Soc. **88**, 1566 (1966).
11. J. Michl, J. Mol. Photochem. **4**, 243 (1972).
12. N.J. Turro, *Modern Molecular Photochemistry* (Benjamin, Menlo Park, California, USA, 1978).
13. Special issue of Chem. Phys. edited by Y. Haas, M. Klessinger, S. Zilberg, 2000.
14. F. Bernardi, M. Olivucci, M.A. Robb, Chem. Soc. Rev. **25**, 321 (1996).
15. M. Garavelli, F. Bernardi, M. Olivucci, T. Vreven, S. Klein, P. Celani, M.A. Robb, Farad. Disc. **110**, 51 (1998).
16. D.R. Cyr, C.C. Hayden, J. Chem. Phys. **104**, 771 (1996).
17. J.S. Baskin, L. Bañares, S. Pedersen, A.H. Zewail, J. Phys. Chem. **100**, 11920 (1996).
18. V. Blanchet, M. Zgierski, T. Seideman, A. Stolow, Nature **401**, 52 (1999).
19. P. Farmanara, V. Stert, W. Radloff, Chem. Phys. Lett. **288**, 518 (1998).
20. J.M. Mestdagh, J.P. Visticot, M. Elhanine, B. Soep, J. Chem. Phys. **113**, 237 (2000).
21. A.J. Merer, R.S. Mulliken, Chem. Rev. **69**, 639 (1969).
22. I. Ohmine, J. Chem. Phys. **83**, 2348 (1985).

23. E.F. Cromwell, A. Stolow, M.J.J. Vrakking, Y.T. Lee, J. Chem. Phys. **97**, 4029 (1992).
24. L. Seidner, W. Domcke, Chem. Phys. **186**, 27 (1994).
25. M. Ben-Nun, T.J. Martínez, Chem. Phys. **259**, 237 (2000).
26. M. Ben-Nun, T.J. Martínez, Chem. Phys. Lett. **298**, 57 (1998).
27. A. Zavriyev, I. Fischer, D.M. Villeneuve, A. Stolow, Chem. Phys. Lett. **234**, 281 (1995).
28. M. Schmitt, S. Lochbrunner, J.P. Shaffer, J.J. Larsen, M.Z. Zgierski, A. Stolow, J. Chem. Phys. **114**, 1206 (2001).
29. W. Fuss, S. Trushin, W. Schmidt, private communication, 2000.
30. W. Fuss, K.L. Kompa, T. Schikarski, W.E. Schmid, S.A. Trushin, Proc. SPIE-Int. Soc. Opt. Eng. **3271**, 114 (1998).
31. H. Bock, H. Borrmann, Z. Havlas, H. Oberhammer, K. Ruppert, A. Simon, Angew. Chem. Int. Ed. Engl. **30**, 1678 (1991).
32. P. Fleurat-Lessard, F. Volatron, J. Phys. Chem. A **102**, 10151 (1998).
33. Y. Nakato, M. Ozaki, H. Tsubomura, Bull. Chem. Soc. Jap. **45**, 1229 (1972).
34. B. Cetinkaya, G.H. King, S.S. Krishnamurthy, M.F. Lappert, J.B. Pedley, Chem. Commun. 1370 (1971).
35. Y. Nakato, J. Phys. Chem. **98**, 7203 (1976).
36. M. Hori, K. Kimura, H. Tsubomura, Spectrochim. Acta A **24**, 1397 (1968).
37. R. Holroyd, S. Ehrenson, J.M. Preses, J. Phys. Chem. **89**, 4244 (1985).
38. W. Rettig, in Electron transfer I, edited by J. Mattay, *Topics in Current Chemistry* (Springer, Berlin, 1994), Vol. 169, p. 253.
39. G. Gregoire, I. Dimicoli, M. Mons, C. DedonderLardeux, C. Jouvet, S. Martrenchard, D. Solgadi, J. Phys. Chem. A **102**, 7896 (1998).
40. R. Holroyd, J. Preses, C. Woody, R. Johnson, Nucl. Instr. Meth. Phys. Res. A **261**, 440 (1987).